

## Density-functional approach to the equation of state of a hard-sphere crystal

A. R. Denton,<sup>1,\*</sup> N. W. Ashcroft,<sup>2</sup> and W. A. Curtin<sup>3</sup>

<sup>1</sup>*Department of Physics, University of Guelph, Guelph, Ontario, Canada N1G 2W1*

<sup>2</sup>*Laboratory of Atomic and Solid State Physics and Materials Science Center, Cornell University, Ithaca, New York 14853-2501*

<sup>3</sup>*Departments of Materials Science and Engineering and Engineering Science and Mechanics, Virginia Polytechnic Institute and State University, Blacksburg, Virginia 24061-0219*

(Received 12 August 1994)

The equation of state (pressure) of a hard-sphere fcc crystal is computed by means of a classical density-functional theory based on the modified weighted-density approximation and a simple Gaussian approximation for the density distribution. Predictions for the total pressure compare favorably with computer simulation data for packing fractions throughout the range  $0.46 < \eta < 0.68$  (i.e., from just below to well above the fluid-solid transition). The ideal-gas and excess contributions are computed *individually* and found to exhibit physically interesting variations with packing fraction. In particular, whereas the ideal-gas pressure is always positive and generally makes the largest contribution, the excess pressure is relatively small and, for  $\eta < 0.63$ , *negative* in sign, implying an *effective attraction* between neighboring hard spheres. Preliminary analysis of available simulation data for mean-square atomic displacements lends support to these predictions. Implications for a recently proposed heuristic model of hard-sphere crystal pressures are also discussed.

PACS number(s): 64.10.+h, 64.30.+t, 61.66.-f, 05.70.Ce

### I. INTRODUCTION

Ever since Ramakrishnan and Yussouff's [1] pioneering theory of the liquid-solid (freezing) transition, the classical density-functional (DF) theory of nonuniform fluids [2-4] has been in a state of rapid evolution. Over the past decade, the theory has been recast in a variety of forms [5-18] and applied to an expanding range of problems in equilibrium statistical mechanics [19]. Applications have included both interfacial systems (e.g., wall-fluid and solid-fluid interfaces), in which spatial variations in the density are generated by external boundary conditions, and bulk systems, which undergo freezing and other phase transitions, in which nonuniformities may arise intrinsically from internal interactions.

In DF studies of crystallization, the bulk crystal is treated as a highly nonuniform system whose density varies on the scale of the lattice constant. To locate the phase transition, the structural and thermodynamic properties of the crystal are usually required only over a narrow range of relatively low metastable and stable densities near liquid-solid coexistence. Beyond the initial focus on freezing transitions, several recent studies have been devoted purely to the stable high-density solid phase alone. Properties examined include the solid density distribution [11,20,21], elastic moduli [22-29], crystal defects [8,30,31], and phonon dispersion [29,32,33].

One basic solid-state property that has not yet been fully examined, but for which DF theory is very well adapted, is the high-density equation of state. The theory is

especially suited to studying the *distribution* of pressure between ideal-gas and excess contributions. In previous work [13], we proposed a "modified weighted-density approximation" (MWDA) and applied it to freezing of the hard-sphere fluid. Our primary interest in that work was in determining freezing parameters and pressures near the transition. The main objective of the present paper is now to extend DF theory, based on the MWDA, to the equation of state of a hard-sphere crystal, at densities well within the stable solid phase, and in the process to examine the relative magnitudes of the ideal-gas and excess contributions to the pressure. An interesting result is that the excess pressure is relatively small in magnitude, and negative in sign, over a considerable range of densities.

In the next section we begin by briefly reviewing the formulation of the MWDA and its application to the equation of state of a crystal. Section III comprises our results for the pressure of a hard-sphere fcc crystal, including the individual ideal-gas and excess contributions, and a comparison with available simulation data. In Sec. IV we discuss the physical meaning of negative excess pressure in a crystal, briefly compare our DF approach with free-volume theory for the hard-sphere equation of state, and consider implications of our results for the physical interpretation of a model recently proposed by Rosenfeld [34]. Finally, in Sec. V we close with a summary and conclusions.

### II. DENSITY-FUNCTIONAL THEORY

The density-functional approach to nonuniform fluids is based on a fundamental variational principle [4], according to which the total Helmholtz free energy functional  $F[\rho]$  is minimized by the equilibrium (spatially varying) one-particle density  $\rho(\mathbf{r})$ , at constant average density. It is standard practice to make the separation

\*Present address: Institut für Theoretische Physik, Technische Universität Wien, Austria.

$$F[\rho] = F_{\text{id}}[\rho] + F_{\text{ex}}[\rho], \quad (1)$$

where the ideal-gas contribution  $F_{\text{id}}[\rho]$  is the free energy of an ideal (noninteracting) nonuniform fluid and the remaining excess contribution  $F_{\text{ex}}[\rho]$  is due entirely to interactions. This separation is usually a matter of convenience, motivated first by the amenability of the excess free energy to rather well-defined approximations, and second by knowledge of the exact relation for the ideal-gas free energy as a functional of the density,

$$\beta F_{\text{id}}[\rho] = \int d\mathbf{r} \rho(\mathbf{r}) \{ \ln[\rho(\mathbf{r})\lambda^3] - 1 \}, \quad (2)$$

where the volume integral extends over all space,  $\lambda$  is the thermal de Broglie wavelength, and  $\beta \equiv 1/k_B T$ . It is important to note, however, that the two contributions may, at least in principle, be *individually* measured experimentally or computed by simulation. In the next section we present evidence suggesting possibly interesting physical significance to this separation.

Guided by its immediate precursor—the weighted-density approximation (WDA) of Curtin and Ashcroft [10]—the MWDA is founded on the basic premise that thermodynamic properties of a nonuniform system (e.g., a solid) may be mapped onto those of an effective uniform fluid. The excess free energy per particle,  $f_{\text{ex}} \equiv F_{\text{ex}}[\rho]/N$ , is thus approximated by

$$f_{\text{ex}} = \frac{F_{\text{ex}}^{\text{MWDA}}[\rho]}{N} = f_0(\hat{\rho}), \quad (3)$$

where  $f_0$  denotes the uniform-fluid counterpart of  $f_{\text{ex}}$ ,  $N$  is the number of particles, and  $\hat{\rho}$  is a weighted density, defined as a weighted average of the physical density  $\rho(\mathbf{r})$  with respect to a weight function  $w$ , according to

$$\hat{\rho} = \frac{1}{N} \int d\mathbf{r} \rho(\mathbf{r}) \int d\mathbf{r}' \rho(\mathbf{r}') w(\mathbf{r} - \mathbf{r}'; \hat{\rho}). \quad (4)$$

Specification of the weight function  $w$  by normalization and by the requirement that the approximate functional  $F_{\text{ex}}^{\text{MWDA}}[\rho]$  yield the exact two-particle direct correlation function  $c_0^{(2)}(|\mathbf{r} - \mathbf{r}'|; \rho)$  in the uniform limit  $[\rho(\mathbf{r}) \rightarrow \rho]$  completes the statement of the MWDA. (For further details, the reader is referred to Ref. [13].)

In our earlier application to freezing of the hard-sphere fluid [13], the predicted freezing parameters—coexisting fluid and solid densities, latent heat, and Lindemann ratio—and solid-phase free energies and pressures were all found to agree well with simulation, generally to within a few percent. In the meantime, several authors [35–37] have attempted to directly apply the MWDA and other “nonperturbative” approximations [14,15] to systems interacting via softer pair potentials [e.g., the Lennard-Jones potential and various inverse-power potentials:  $\phi(r) \sim (\sigma/r)^n$ , where  $n$  tunes the softness of the potential]. They have come to the conclusion that for such systems these approximations actually are considerably less successful, in some cases even failing to predict a freezing transition.

The source of this inconsistency is likely to be found in the treatment of higher-order correlations. Indeed, by extending the MWDA to fully incorporate third-order

correlations, together with approximate higher-order correlations, Likos and Ashcroft have recently obtained accurate freezing parameters for both the hard-sphere system [17] ( $n = \infty$ ) and the one-component plasma [18] ( $n = 1$ ), the hardest and the softest, respectively, of the inverse-power potentials. We caution, therefore, that extension of the present application to other potentials may require implementation of a more accurate version of DF theory, such as the extended MWDA [17,18].

In freezing studies, the solid is usually assumed to be a perfect crystal (i.e., no vacancies or interstitials), although in a few studies [8,31] a mean vacancy concentration has been allowed by treating the number of atoms per unit cell as a free parameter. Furthermore, on the basis of simulation evidence for harmonic atomic motions [38,39], the crystal density distribution is often parametrized in real space as a sum of normalized Gaussians centered on the sites of an *assumed* Bravais lattice [6,40], according to

$$\rho(\mathbf{r}) \equiv \left[ \frac{\alpha}{\pi} \right]^{3/2} \sum_{\mathbf{R}} e^{-\alpha|\mathbf{r} - \mathbf{R}|^2}, \quad (5)$$

where  $\mathbf{R}$  denotes the position vector of a lattice site, and  $\alpha$  is the Gaussian width parameter, which is directly related to the Debye-Waller factor commonly measured in solids. For comparison with this simple Gaussian approximation, several authors have experimented with more realistic (and complicated) parametrizations. For example, Laird, McCoy, and Haymet [20] have employed a Fourier component representation of  $\rho(\mathbf{r})$ , Colot, Baus, and Xu [41] and Curtin and Runge [42] have examined anisotropic variants of Eq. (5), and Popović and Jarić [43] have generalized Eq. (5) to an *arbitrary* Bravais lattice with a symmetric Gaussian width matrix. In general, the freezing parameters of the hard-sphere fluid are found to be rather insensitive to the choice of parametrization. Simulation studies by Young and Alder [38] and Ohnesorge, Löwen, and Wagner [21] have demonstrated the form of the hard-sphere crystal density distribution to be close to Gaussian, especially near close packing. At lower densities near melting, however, the tails of the distribution do exhibit significant anisotropic deviations of roughly 10% from the Gaussian form [21].

Given a density parametrization, the weighted density is computed by iteratively solving the implicit relation

$$\hat{\rho} = \rho - \frac{\Theta(\rho, \alpha, \hat{\rho})}{\rho} f'_0(\hat{\rho}), \quad (6)$$

where  $\rho$  is the average solid density and

$$\Theta(\rho, \alpha, \hat{\rho}) \equiv \frac{1}{2} \sum_{\mathbf{G} \neq 0} \rho_{\mathbf{G}}^2(\rho, \alpha) c_0^{(2)}(\mathbf{G}, \hat{\rho}) \quad (7)$$

is the contribution that clearly depends on the crystal structure of the solid (i.e., the lattice symmetry and the distribution of the one-particle density about the lattice sites). In Eq. (7),  $\rho_{\mathbf{G}}(\rho, \alpha) = \rho \exp(-G^2/4\alpha)$  is  $\rho$  times the Fourier component at reciprocal-lattice vector (RLV)  $\mathbf{G}$  of the Gaussian single-site density, and  $c_0^{(2)}(\mathbf{G}, \hat{\rho})$  is the Fourier component at RLV  $\mathbf{G}$  of the two-particle direct correlation function of the uniform fluid of *effective* density  $\hat{\rho}$ . If the Gaussians are assumed to be

nonoverlapping—a valid assumption for the hard-sphere system at densities near and above the freezing transition—then the ideal-gas free energy per particle,  $f_{\text{id}} \equiv F_{\text{id}}/N$ , can be well approximated by

$$\beta f_{\text{id}}(\alpha) = \frac{3}{2} \ln(\alpha) + \text{const.} \quad (8)$$

Taken together, Eqs. (3), (6), (7), and (8) constitute a well-defined approximation for the functional  $F[\rho]$  which, when minimized with respect to the single variational parameter  $\alpha$ , at fixed average density, yields the Helmholtz free energy of the crystal.

At fixed temperature, the total pressure  $P$  of the crystal—our main concern in this paper—can be derived from the total free energy per particle,  $f = f_{\text{id}} + f_{\text{ex}}$ , according to

$$\frac{\beta P}{\rho} = \beta \rho \frac{\partial}{\partial \rho} f(\rho, \alpha) = \frac{3\rho}{2\alpha} \frac{\partial \alpha}{\partial \rho} + \beta \rho f'_{\text{ex}}(\rho), \quad (9)$$

from which two distinct contributions to the total pressure can be identified. The first, the “ideal-gas pressure”  $P_{\text{id}}$ , is given by

$$\frac{\beta P_{\text{id}}}{\rho} = \frac{3\rho}{2\alpha} \frac{\partial \alpha}{\partial \rho}, \quad (10)$$

and the second, the “excess pressure”  $P_{\text{ex}}$ , by

$$\frac{\beta P_{\text{ex}}}{\rho} = \beta \rho f'_{\text{ex}}(\rho) = \beta \rho f'_{\text{ex}}(\hat{\rho}) \hat{\rho}'(\rho). \quad (11)$$

Note that both contributions depend on the structure of the solid through the Gaussian width parameter  $\alpha$  and the lattice symmetry.

### III. APPLICATION TO A HARD-SPHERE CRYSTAL

For several reasons, many of the early applications of DF theory focused on systems interacting via the hard-sphere pair potential. Since structural properties of dense fluids are known to be governed largely by short-range repulsive interactions [44,45], hard-sphere systems are of fundamental importance as they permit effects of the most singular possible repulsions to be studied in isolation from competing attractive interactions. Moreover, the hard-sphere potential is especially relevant to dense solids where short-range repulsive interactions predominate. From a practical perspective, structural and thermodynamic properties of the uniform hard-sphere fluid, which are required as input to the theory, are well understood and readily available in convenient analytic form. Finally, extensive computer simulation data for hard-sphere systems [39] permit systematic testing of theoretical predictions.

Here the requisite uniform-state functions, namely, the excess free energy per particle  $f_0$  and the direct correlation function  $c_0^{(2)}$  [see Eqs. (6) and (7)], are obtained directly from the analytic solution of the Percus-Yevick integral equation for hard spheres [46,47]. We have also explored the use of the more accurate Verlet-Weis [48] functions, and in Sec. IV we discuss the sensitivity of the results to the choice of input functions.

By implementing the MWDA, adopting the simple

Gaussian approximation for the density distribution, and numerically evaluating the derivatives in Eq. (9), we have computed the total pressure  $\beta P/\rho$  of a hard-sphere crystal with fcc lattice symmetry, as well as the individual ideal-gas and excess contributions. The results are plotted in Fig. 1, and tabulated in Table I, as a function of crystal packing fraction  $\eta = (\pi/6)\rho\sigma^3$  from  $\eta = 0.46$ , the lower limit of mechanical stability, to  $\eta = 0.71$  (cf. the close-packed limit  $\eta_0 = \sqrt{2}\pi/6 \simeq 0.74$ ). The total pressure increases monotonically, rising sharply as  $\eta$  nears close packing. More interesting is the behavior of the individual ideal-gas and excess contributions. The ideal-gas pressure is evidently always positive and, except for a narrow range at the lowest stable packing fractions ( $0.46 < \eta < 0.51$ ), a monotonically increasing function of  $\eta$ , which simply reflects the monotonic increase of  $\alpha$  with  $\eta$  [see Eq. (10)]. Furthermore,  $P_{\text{id}}$  clearly makes the dominant contribution to  $P$  except at the highest packing fractions. In contrast, the excess pressure is *negative* and comparatively small in magnitude at lower packing fractions in the range  $0.46 < \eta < 0.63$ . At  $\eta \simeq 0.63$ , however,  $P_{\text{ex}}$  changes sign and thereafter increases rapidly as the close-packed limit is approached.

Figure 1 includes, for comparison, the simulation data of Hoover and co-workers [49] for the total pressure (see Table II), which are seen to be in generally good agreement with theory, except above  $\eta \simeq 0.68$  where the theory increasingly overestimates the pressure. Also included are limited data for the individual ideal-gas and excess pressures, obtained by analyzing the simulation data of Young and Alder [38] for mean-square atomic displacements  $\langle r^2 \rangle$ . As shown in Table III, theory and simulation are in generally fair agreement for  $\langle r^2 \rangle$  over a range of packing fractions, although the theory consistently overestimates atomic localization. Since the solid density appears to be reasonably well described by the Gaussian approximation, in which  $\langle r^2 \rangle = (3/2\alpha)$ , Young and Alder’s data for  $\langle r^2 \rangle$  may easily be converted to equivalent Gaussian widths  $\alpha$ . Then, by fitting a sim-

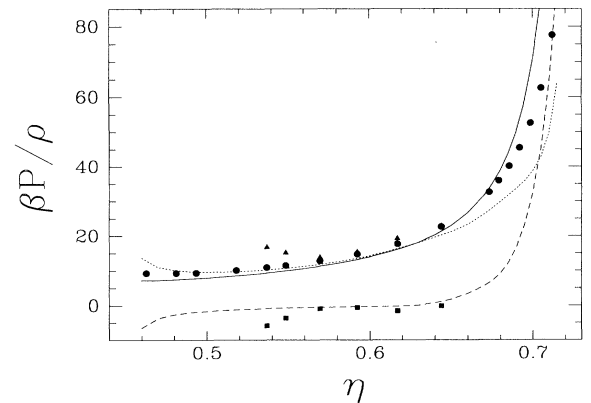


FIG. 1. Equation of state  $\beta P/\rho$  vs average packing fraction  $\eta$  for a hard-sphere fcc crystal. Solid, dotted, and dashed curves are the total, ideal-gas, and excess contributions, respectively, predicted by DF theory (MWDA). Circles, triangles, and squares represent (in the same order) corresponding simulation data [38,49] (see text).

TABLE I. Total, ideal-gas, and excess contributions to the equation of state  $\beta P/\rho$  for a hard-sphere fcc crystal vs average packing fraction  $\eta$ , as predicted by DF theory (MWDA), corresponding to Fig. 1. Also included are various localization parameters,  $\alpha$ ,  $L$ , and  $s$  (see text for definitions).

$\eta$	$\beta P/\rho$	$\beta P_{id}/\rho$	$\beta P_{ex}/\rho$	$\alpha\sigma^2$	$L$	$s$
0.46	7.21	13.7	-6.48	40.33	0.165	1.12
0.47	7.26	11.0	-3.77	47.95	0.152	1.08
0.48	7.41	10.1	-2.70	55.57	0.142	1.06
0.49	7.62	9.70	-2.08	63.65	0.134	1.04
0.50	7.88	9.57	-1.69	72.47	0.126	1.03
0.51	8.20	9.58	-1.38	82.23	0.119	1.02
0.52	8.56	9.75	-1.19	93.20	0.113	1.01
0.53	8.97	10.0	-1.04	105.6	0.107	1.01
0.54	9.44	10.3	-0.86	119.9	0.101	1.01
0.55	9.97	10.7	-0.74	136.3	0.095	1.01
0.56	10.6	11.2	-0.64	155.5	0.089	1.01
0.57	11.2	11.8	-0.54	178.1	0.084	1.01
0.58	12.0	12.5	-0.47	204.9	0.079	1.01
0.59	12.9	13.3	-0.40	237.3	0.074	1.01
0.60	13.9	14.2	-0.33	276.8	0.069	1.01
0.61	15.1	15.4	-0.28	325.8	0.064	1.02
0.62	16.5	16.7	-0.19	387.5	0.059	1.02
0.63	18.1	18.1	0.06	466.2	0.054	1.03
0.64	20.2	19.5	0.68	568.0	0.049	1.03
0.65	22.9	21.2	1.78	700.7	0.044	1.04
0.66	26.6	23.2	3.36	877.7	0.040	1.06
0.67	31.6	26.1	5.49	1123	0.035	1.08
0.68	38.8	29.8	9.08	1480	0.031	1.11
0.69	50.3	33.6	16.7	2014	0.027	1.15
0.70	70.8	38.6	32.2	2840	0.023	1.21
0.71	114	50.0	63.9	4273	0.018	1.33

ple fifth-order polynomial to  $\ln\alpha$  vs  $\eta$ , as illustrated in Fig. 2, and computing the derivative  $d\ln\alpha/d\eta$ , we have determined  $P_{id}$  from Eq. (10), and then  $P_{ex}$  as the difference,  $P_{ex} = P - P_{id}$ . The resulting data for  $P_{id}$  and  $P_{ex}$  are seen to be in fair agreement with our predictions.

Although this simple test, using available simulation

data, appears to support the predicted distribution between ideal-gas and excess pressures, a more conclusive test will require more detailed information about the one-particle density, particularly its second moment. In passing, we note that a similar procedure could, in principle, also be applied to experimental Debye-Waller factors

TABLE II. Equation of state  $\beta P/\rho$  vs free-volume parameter  $(V - V_0)/V_0$ , where  $V_0$  is the close-packed volume, as predicted by DF theory (MWDA) and compared with molecular dynamics (MD) simulation data [49] and free-volume (FV) theory [Eq. (14)].

$(V - V_0)/V_0$	$\eta$	$(\beta P/\rho)_{MWDA}$	$(\beta P/\rho)_{MD}$	$(\beta P/\rho)_{FV}$
0.60	0.4628	7.21	9.315	6.896
0.5385	0.4813	7.43	9.253	7.476
0.50	0.4937	7.71	9.304	7.910
0.4286	0.5183	8.50	10.088	8.921
0.3793	0.5368	9.29	10.870	9.838
0.35	0.5485	9.89	11.452	10.505
0.30	0.5696	11.2	12.801	11.942
0.25	0.5924	13.1	14.736	13.950
0.20	0.6171	16.0	17.683	16.960
0.15	0.6439	21.2	22.640	21.969
0.10	0.6732	33.6	32.605	31.979
0.09	0.6793	38.3	35.932	35.314
0.08	0.6856	44.6	40.093	39.483
0.07	0.6920	53.5	45.445	44.842
0.06	0.6986	67.0	52.582	51.987
0.05	0.7052	88.8	62.577	61.989
0.04	0.7120	128	77.573	76.991

TABLE III. Mean-square atomic displacement  $\langle(r/\sigma)^2\rangle$  for several average packing fractions  $\eta$ , as predicted by DF theory (MWDA) and compared with available MD simulation data [38].

$(V-V_0)/V_0$	$\eta$	$10^3\langle(r/\sigma)^2\rangle_{\text{MWDA}}$	$10^3\langle(r/\sigma)^2\rangle_{\text{MD}}$
0.42	0.5215	15.80	26.0±0.6
0.3488	0.5506	10.92	15.6±0.3
0.25	0.5924	6.10	7.81±0.11
0.20	0.6171	4.08	4.89±0.12
0.15	0.6439	2.44	2.68±0.03

for dense crystals. In cases where the Gaussian approximation is not valid, however, more extensive knowledge of the one-particle density distribution may be required to compute  $F_{\text{id}}$  by numerical integration via Eq. (2), and then  $P_{\text{id}}$  as its density derivative.

The physical significance of negative excess pressure is discussed in the following section. Some insight into its origin in the theory, however, is gained by considering two localization parameters,  $L$  and  $s$ , derived from the Gaussian width parameter  $\alpha$ , and included in Table I. The first is simply a generalization of the usual Lindemann ratio, defined as the ratio of the rms displacement  $\langle r^2 \rangle^{1/2}$  of an atom away from its equilibrium lattice site in the crystal to the mean distance  $d$  between the centers of nearest neighbors. The second, which we call the “separation ratio,” is defined as the ratio of  $\langle r^2 \rangle^{1/2}$  to the mean distance  $(d-\sigma)$  separating nearest neighbors from contact. (It can be shown, incidentally, that  $\langle r^2 \rangle^{1/2}$  is just  $1/\sqrt{2}$  times the standard deviation of the distance between nearest neighbors.) For a fcc lattice,

$$L \equiv \frac{\langle r^2 \rangle^{1/2}}{d} = \left[ \frac{3}{\alpha\sigma^2} \right]^{1/2} \left[ \frac{3\eta}{2\pi} \right]^{1/3} \quad (12)$$

and

$$s \equiv \frac{\langle r^2 \rangle^{1/2}}{d-\sigma} = \left[ \frac{3}{\alpha\sigma^2} \right]^{1/2} \left[ \left[ \frac{2\pi}{3\eta} \right]^{1/3} - 2^{-1/2} \right]^{-1}. \quad (13)$$

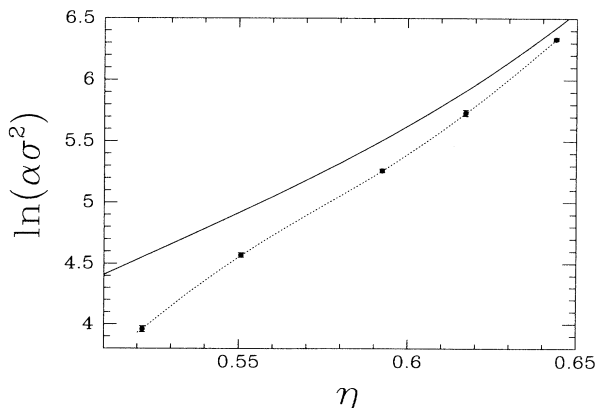


FIG. 2. Polynomial fit (dotted curve) to equivalent Gaussian width parameter  $\alpha$  (see text) derived from simulation data [38] (dots), together with DF theory predictions (solid curve), vs average packing fraction  $\eta$ .

From Table I, the Gaussian width parameter  $\alpha$  is seen to increase monotonically with packing fraction, and correspondingly the generalized Lindemann ratio  $L$  decreases monotonically, simply reflecting the increasing localization of the atoms about their equilibrium lattice sites as the crystal is compressed. More illuminating is the separation ratio  $s$ , which is relatively constant and close to unity, except at either end of the  $\eta$  range where it is slightly larger. This indicates that over a wide range of packing fractions the rms displacement of an atom generally remains comparable to the mean distance separating it from contact with its neighbors. Furthermore, the initial decrease in  $s$  with increasing  $\eta$  reflects a diminishing overlap of neighboring density distributions, which in turn implies a decreasing weighted density  $\hat{\rho}$  [see Eq. (4) and also Fig. 5, discussed below] and hence [from Eq. (11)] a negative excess pressure. Similarly, the relatively weak variation of  $s$  with  $\eta$  implies a correspondingly weak variation of  $\hat{\rho}$ , which accounts [again from Eq. (11)] for the small magnitude of  $P_{\text{ex}}$ .

#### IV. DISCUSSION

As mentioned in Sec. III, we have tested the sensitivity of our DF results to the accuracy of the fluid-state input data by repeating some of the calculations using the more accurate Verlet-Weis [48] input functions in place of the Percus-Yevick functions. In general, with the Verlet-Weis input the Gaussian width parameter is found to be slightly lower—typically by no more than 10% for  $\eta < 0.6$ , but more so for higher  $\eta$ . Correspondingly, the pressures are also slightly lower—making the comparison with simulation slightly worse at lower  $\eta$ , but better at higher  $\eta$ —although the qualitative dependence on  $\eta$  is unchanged.

In the equation of state results presented in Fig. 1 two features stand out: (1) the small negative values of the excess contribution, and (2) the dominance of the ideal-gas contribution at all but the highest packing fractions. The magnitude of  $P_{\text{ex}}$  indicates weak interactions between neighboring hard spheres, which is ensured by their strong localization. The reason for such strong localization is well understood on the basis of competing contributions to the free energy, which for hard-sphere systems is purely entropic [50]. In a crystal the loss in global (or configurational) entropy resulting from localization of the atoms to within the vicinity of lattice sites is more than balanced by a corresponding gain in local entropy as each sphere enjoys access to a larger (local) free volume. The rapid increase in  $P_{\text{ex}}$  near close packing results from the inevitable loss of free volume—and attendant cost in local entropy—as neighboring hard spheres are squeezed ever closer together. In passing, it is of interest to note that three centuries ago, well before the development of kinetic theory, Newton conceived of the pressure of a fluid as a purely static property arising solely from short-range repulsive interactions between neighboring atoms [51]. Our DF theory results suggest that indeed—at least in the solid phase—such interactions *can* make a significant contribution to the pressure, albeit only very near to the close-packed limit.

The negative sign of  $P_{\text{ex}}$  may be physically interpreted as implying an *effective hard-sphere attraction*, due to interactions only, that opposes ideal-gas repulsions. This is manifested by the tendency, noted above, of the density distribution to contract (become narrower)—beyond what would be expected from the lattice contraction alone—as the packing fraction increases. It is interesting to compare this behavior of the classical hard-sphere crystal with that of its *quantum* counterpart. In a similar DF analysis of the ground-state quantum freezing transition [52], it was shown that for a Bose hard-sphere crystal near freezing the weighted density actually *increases* monotonically with packing fraction. This, in turn, implies a strictly *positive* excess pressure in the quantum system, differing qualitatively from the classical case. The difference can be attributed to quantum zero-point energy, which tends to strongly oppose localization. This can be seen from the *linear* dependence of the quantum ideal-gas ground-state energy on  $\alpha$  [52], as compared with the much weaker logarithmic dependence of the classical ideal-gas free energy [Eq. (8)].

The notion of effective *attractive* interactions in hard-sphere systems is by no means original. For instance, Shinomoto [53] has invoked this notion in deriving an equation of state for the one-component hard-sphere fluid. More recently, Biben and Hansen [54], by means of an integral-equation analysis of additive binary hard-sphere fluid mixtures, and Kaplan *et al* [55], in an experimental study of binary colloidal mixtures, have addressed the issue of phase separation in hard-sphere mixtures. For highly asymmetric mixtures, with diameter ratios smaller than roughly 0.2, phase separation was seen to occur in both studies, and was attributed to an effective attraction or “stickiness” between the larger spheres, mediated by the smaller spheres. In light of the connection that we have identified between excess pressure and effective attraction, we suggest that it may also be worth examining excess contributions to the three pair pressures (associated with each of the three pair interactions) of binary hard-sphere mixtures for possible signals of phase separation. It should be noted, however, that the effective attraction has different physical origins in fluids and crystals, being determined in fluids by global excluded volume, but in crystals by local excluded volume.

The DF approach to the equation of state may be compared with the well-known free-volume theory [56]. The latter begins by partitioning the system into  $N$  cells and then makes two essential approximations: (1) single occupancy of the cells and (2) independent (uncorrelated) motions of the atoms within their cells. For a  $D$ -dimensional hard-sphere fcc crystal the theory predicts the equation of state

$$\frac{\beta P}{\rho} = \left[ 1 - \left( \frac{\eta}{\eta_0} \right)^{1/D} \right]^{-1}, \quad (14)$$

where  $\eta_0$  is the close-packed limit of  $\eta$ . Despite its analytic simplicity, Eq. (14) is also remarkably accurate at high density, as Fig. 3 and Table II illustrate. This is perhaps not surprising though, considering that the two underlying approximations of the theory are well

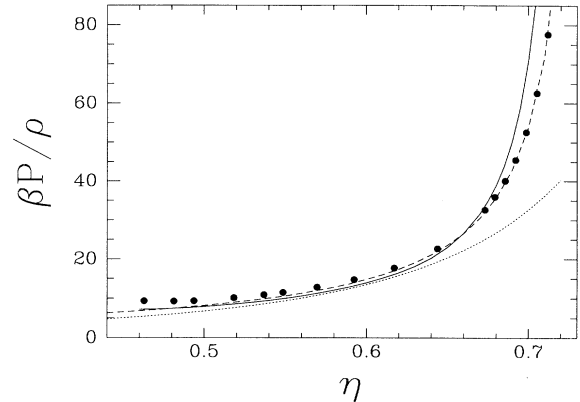


FIG. 3. Equation of state  $\beta P/\rho$  vs average packing fraction  $\eta$ , as predicted by DF theory (solid curve) and compared with simulation data [49] (dots), free-volume theory [Eq. (14)] (dashed curve), and Rosenfeld’s model [34] (dotted curve).

justified—and increasingly so with increasing  $\eta$ —by the structural properties of the hard-sphere crystal predicted by DF theory, namely, the extreme localization of the atoms about their lattice sites and the resulting weak interaction between neighbors. It is important to note, however, that this structural information is not given by free-volume theory itself, but must be assumed *a priori*. Furthermore, the theory does not permit the separation of pressure into ideal-gas and excess contributions, and thus offers less physical insight than DF theory into the properties of the crystal.

Finally, to further demonstrate the importance of the pressure distribution, we compare our DF results with the predictions of a heuristic model recently proposed by Rosenfeld [34], which we first briefly summarize. The model is based on the observation that the same structure-dependent quantity  $\Theta$  that appears in the formulation of the MWDA [Eqs. (6) and (7)] also appears in the effective liquid approximation (ELA) of Baus and Colot [7]. The ELA for the excess Helmholtz free energy per particle of the solid phase may be expressed in the form

$$f_{\text{ex}} = f_0(\rho) - \frac{\Theta(\rho, \alpha, \bar{\rho})}{\beta \rho}, \quad (15)$$

where  $\bar{\rho}$  is the density of an effective uniform liquid. The effective density  $\bar{\rho}$  was originally prescribed [7] by a physically motivated structural criterion, which subsequently was shown by Colot, Baus, and Xu [41] to be empirically equivalent to the variational criterion

$$\frac{\partial}{\partial \bar{\rho}} \Theta(\rho, \alpha, \bar{\rho}) = 0. \quad (16)$$

The derivation of Rosenfeld’s model is based on the key assumption that an analogous variational criterion exists for the MWDA of the form

$$\frac{\partial}{\partial \hat{\rho}} \Theta(\rho, \alpha, \hat{\rho}) = 0, \quad (17)$$

the difference being the appearance of  $\hat{\rho}$  rather than  $\bar{\rho}$ .

Supposing this to be so, and proceeding to substitute Eq. (6) into Eq. (17), then yields the following relation for  $\hat{\rho}$  [Eq. (12b) in Ref. [34]]:

$$\hat{\rho} = \rho - \frac{f'_0(\hat{\rho})}{f''_0(\hat{\rho})}. \quad (18)$$

Taken together, Eqs. (3) and (18) constitute an approximation for the solid-phase excess free energy per particle  $f_{\text{ex}}$ . It should be noted, however, that this approximation is entirely independent of the crystal structure of the solid. This is despite the fact that on physical grounds the excess free energy of a solid must depend not only on the average density, but also on structural details of the density profile  $\rho(\mathbf{r})$ , since otherwise there clearly would exist no basis for distinguishing the relative stabilities of different crystal structures.

Proceeding further, by assuming that

$$\Theta(\rho, \alpha, \bar{\rho}) = \Theta(\rho, \alpha, \hat{\rho}), \quad (19)$$

and thus implicitly assuming the equivalence of the effective density  $\bar{\rho}$  and the weighted density  $\hat{\rho}$ , an assumption which we examine in some detail below,  $\Theta$  is eliminated between Eqs. (6) and (15) to obtain another relation [Eq. (13) in Ref. [34]],

$$f_{\text{ex}}(\rho) = f_0(\rho) + f'_0(\hat{\rho})(\hat{\rho} - \rho), \quad (20)$$

which, together with Eq. (18), constitutes a second structure-independent approximation for  $f_{\text{ex}}$ .

From Eqs. (3), (11), (18), and (20), one obtains corresponding structure-independent approximations for the excess pressure. Since the model eliminates *a priori* any structural information for the solid, there is, however, no obvious choice for a structure-dependent ideal-gas pressure. Instead, motivated by a formal resemblance between the equation of state of a solid and that of a uniform fluid, Rosenfeld adopts the following model equation of state:

$$\frac{\beta P}{\rho} = 1 + \rho f'_{\text{ex}}(\rho), \quad (21)$$

in which the ideal-gal contribution is that of a uniform fluid.

For comparison with the predictions of the MWDA, we show in Fig. 4 the variation with packing fraction of the ideal-gas, excess, and total pressures as calculated from Eqs. (3), (18), and (21). Rosenfeld's model is seen to predict an excess pressure that is always positive and one that *dominates* the trivially constant ideal-gas pressure, in direct contrast to the predictions of the MWDA (see Fig. 1). Remarkably, however, by what appears to be a fortuitous cancellation of errors between the ideal-gas and excess pressures in Eq. (21), the *total* pressure is actually a physically sensible function of packing fraction (see Fig. 3).

The apparently unphysical distribution of pressure between the ideal-gas and excess contributions in Rosenfeld's model can be traced to the assumption, implicit in the derivation of the model, that the weighted density  $\hat{\rho}$  in the MWDA and the effective density  $\bar{\rho}$  in the ELA are similar quantities. Actually,  $\hat{\rho}$  and  $\bar{\rho}$  exhibit

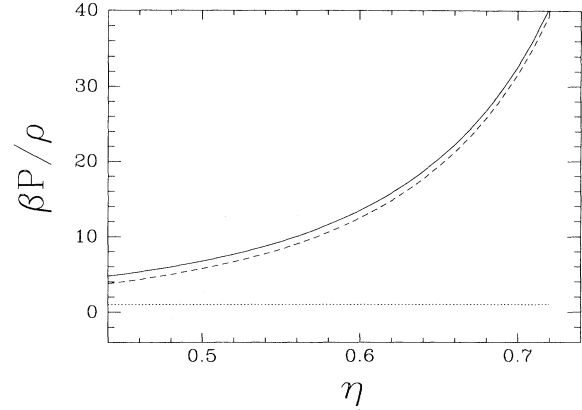


FIG. 4. Equation of state  $\beta P/\rho$  vs average packing fraction  $\eta$ , as predicted by Rosenfeld's model [34] (independent of crystal structure). Curves have the same meaning as in Fig. 1.

qualitatively different variations with packing fraction. As Fig. 5 illustrates,  $\hat{\rho}$  is a *decreasing* function of  $\eta$  from  $\eta \approx 0.46$  through the freezing transition, reaching a minimum at  $\eta \approx 0.63$  and thereafter increasing monotonically with  $\eta$ . In contrast,  $\bar{\rho}$  is everywhere a monotonically *increasing* function of  $\eta$  [41], and is always considerably larger than  $\hat{\rho}$ .

The qualitatively different behaviors of  $\hat{\rho}$  in the MWDA and  $\bar{\rho}$  in the ELA preclude the application of a variational criterion to the MWDA [Eq. (17)], as well as the subsequent equating of  $\Theta(\rho, \alpha, \bar{\rho})$  and  $\Theta(\rho, \alpha, \hat{\rho})$  [Eq. (19)]. This is further demonstrated by a direct comparison of the variation with  $\eta$  of  $\hat{\rho}$  in the MWDA [Eq. (6)] and  $\bar{\rho}$  in Rosenfeld's model [Eq. (18)], also illustrated in Fig. 5. Evidently,  $\hat{\rho}$  in Rosenfeld's model is quite a different quantity from  $\bar{\rho}$  in the MWDA. This comparison demonstrates that the underlying premise of Rosenfeld's model, namely, the essential equivalence of  $\hat{\rho}$  and  $\bar{\rho}$ , as embodied in Eqs. (17) and (19), is actually in-

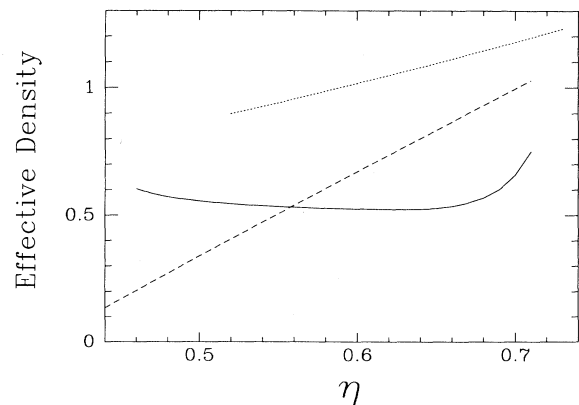


FIG. 5. Effective density vs average packing fraction  $\eta$  as predicted by DF theory (with a fcc crystal lattice and a Gaussian density profile) and by Rosenfeld's model [34] (independent of crystal structure). Solid curve:  $\hat{\rho}\sigma^3$  in the MWDA; dotted curve:  $\bar{\rho}\sigma^3$  in the ELA [41]; dashed curve:  $\hat{\rho}\sigma^3$  in Rosenfeld's model.

consistent with results derived from it.

The inconsistency demonstrated above has implications for a major conclusion of Ref. [34] regarding a possible connection between three different versions of DF theory. By demonstrating that the relations for  $f_{\text{ex}}$  expressed by Eqs. (3), (18), and (20), as well as a third relation suggested to be associated with the generalized effective liquid approximation (GELA) [15], may all be obtained by a "trivial parabola-shift" transformation between  $f_0$  and  $f_{\text{ex}}$ , Rosenfeld concludes that the three versions of DF theory based on the MWDA, the ELA, and the GELA may all be similarly related in their application to freezing of the hard-sphere system. Since, however, the excess free energy per particle of the hard-sphere fluid  $f_0$  is a monotonically increasing function of packing fraction, it follows from Eq. (3) that the behavior of  $f_{\text{ex}}$  in the MWDA differs from that in Rosenfeld's model in a manner analogous to the difference in  $\hat{\rho}$ . Thus, whereas the MWDA predicts  $f_{\text{ex}}$  to be a *decreasing* function of  $\eta$  for  $\eta \leq 0.63$ , Rosenfeld's model predicts it to be an *increasing* function (see Fig. 1 of Ref. [34]). These qualitative differences between Rosenfeld's approximations for the excess free energy per particle and the actual DF approximations from which they are derived leave inconclusive, in our judgment, the issue of possible connections between different versions of DF theory.

## V. SUMMARY AND CONCLUSIONS

In summary, we have used classical density-functional theory, in a form based on the modified weighted-density approximation and a Gaussian approximation for the density distribution, to compute the equation of state (pressure) of a hard-sphere fcc crystal at densities ranging from near to well above the fluid-solid transition. The predicted total pressure increases monotonically with packing fraction, in good agreement with simulation data at all but the highest packing fractions.

The individual ideal-gas and excess contributions exhibit far more interesting behavior. In particular, the ideal-gas pressure is always positive, generally dominant, and increases monotonically with packing fraction above freezing. Conversely, the excess pressure is relatively small in magnitude and initially negative in sign, but becomes positive and increases monotonically with increasing rapidity as the close-packed limit is approached. The negative sign of the excess pressure would suggest an effective attraction between hard spheres, entirely attributable to interactions, that opposes ideal-gas repulsions and is manifested in the rapid localization of the atoms about their lattice sites as the crystal is compressed.

Although the distribution between ideal-gas and excess pressures appears to be at least qualitatively supported by

preliminary analysis of available simulation data, the possibility remains that, given the small magnitude of the excess pressure, the sign is merely an artifact of theoretical approximations, principally the MWDA for the excess free energy and the Gaussian approximation for the density distribution. Indeed, there is already some evidence that the extended MWDA of Likos and Ashcroft predicts a weighted density that *increases* with average solid density in the range  $1.0 \lesssim \rho\sigma^3 \lesssim 1.1$ , which would imply a *positive* excess pressure over the same range (see Fig. 1 and Table IV of Ref. [18]). We suggest that the predicted pressure distribution can be more conclusively tested via simulation by a careful characterization of the density distribution, particularly its second moment. Such data would also serve to guide the design of more accurate density parametrizations.

Compared with the simple free-volume theory, the DF approach is quantitatively less accurate in predicting the total pressure at high densities, but provides additional structural information in the form of localization parameters. Furthermore, free-volume theory cannot resolve the individual ideal-gas and excess pressures.

Finally, we have considered the implications of our findings for the physical significance of a model recently proposed by Rosenfeld. Compared with DF theory, Rosenfeld's model predicts a qualitatively different distribution between ideal-gas and excess pressures, a discrepancy that may be attributed to two approximations of the model: (1) an apparently inappropriate mixing of two independent versions of DF theory based on different approximations, and (2) an oversimplified treatment of the ideal-gas pressure. It follows that conclusions drawn from the model regarding a possible connection between different versions of DF theory in applications to hard-sphere freezing are unsupported. This does not negate, of course, the possibility that since non-perturbative DF approximations, such as the MWDA, ELA, and GELA, are all related by a common basic assumption—namely, that thermodynamic and structural functionals for the nonuniform solid may be mapped onto the corresponding functions for the uniform fluid—deeper connections between the various approximations may yet be discovered. This is an interesting issue fully deserving of further consideration.

## ACKNOWLEDGMENTS

This work was supported in part by the National Science Foundation through the Materials Science Center at Cornell University, Grant No. DMR-91-21654. One of us (A.R.D.) gratefully acknowledges financial support from the Natural Sciences and Engineering Research Council of Canada during the early stages of the work.

- 
- [1] T. V. Ramakrishnan and M. Yussouff, *Phys. Rev. B* **19**, 2775 (1979).  
 [2] F. H. Stillinger and F. P. Buff, *J. Chem. Phys.* **37**, 1 (1962).  
 [3] J. L. Lebowitz and J. K. Percus, *J. Math. Phys.* **4**, 116 (1963).  
 [4] N. D. Mermin, *Phys. Rev.* **137**, A1441 (1965); R. Evans,

- Adv. Phys.* **28**, 143 (1979).  
 [5] A. D. J. Haymet and D. J. Oxtoby, *J. Chem. Phys.* **74**, 2559 (1981).  
 [6] P. Tarazona, *Mol. Phys.* **52**, 81 (1984); *Phys. Rev. A* **31**, 2672 (1985).  
 [7] M. Baus and J. L. Colot, *Mol. Phys.* **55**, 653 (1985).

- [8] G. L. Jones and U. Mohanty, *Mol. Phys.* **54**, 1241 (1985).
- [9] T. F. Meister and D. M. Kroll, *Phys. Rev. A* **31**, 4055 (1985).
- [10] W. A. Curtin and N. W. Ashcroft, *Phys. Rev. A* **32**, 2909 (1985); *Phys. Rev. Lett.* **56**, 2775 (1986).
- [11] F. Iglói and J. Hafner, *J. Phys. C* **19**, 5799 (1986).
- [12] R. D. Groot and J. P. van der Eerden, *Phys. Rev. A* **36**, 4356 (1987).
- [13] A. R. Denton and N. W. Ashcroft, *Phys. Rev. A* **39**, 4701 (1989).
- [14] M. Baus, *J. Phys. Condens. Matter* **1**, 3131 (1989).
- [15] J. F. Lutsko and M. Baus, *Phys. Rev. Lett.* **64**, 761 (1990); *Phys. Rev. A* **41**, 6647 (1990).
- [16] Y. Rosenfeld, *Phys. Rev. Lett.* **63**, 980 (1989).
- [17] C. N. Likos and N. W. Ashcroft, *Phys. Rev. Lett.* **69**, 316 (1992); **69**, 3134(E) (1992).
- [18] C. N. Likos and N. W. Ashcroft, *J. Chem. Phys.* **99**, 9090 (1993).
- [19] For recent reviews of classical density-functional theory and its applications, see H. Löwen, *Phys. Rep.* **237**, 249 (1994); R. Evans, in *Inhomogeneous Fluids*, edited by D. Henderson (Dekker, New York, 1992); Y. Singh, *Phys. Rep.* **207**, 351 (1991); D. W. Oxtoby, in *Liquids, Freezing, and the Glass Transition*, Les Houches Session 51, edited by J.-P. Hansen, D. Levesque, and J. Zinn-Justin (Elsevier, New York, 1990); M. Baus, *J. Phys. Condens. Matter* **2**, 2111 (1990); R. Evans, in *Liquids at Interfaces*, Les Houches Session 48, edited by J. Charvolin, J. F. Joanny, and J. Zinn-Justin (Elsevier, New York, 1989).
- [20] B. B. Laird, J. D. McCoy, and A. D. J. Haymet, *J. Chem. Phys.* **87**, 5449 (1987).
- [21] R. Ohnesorge, H. Löwen, and H. Wagner, *Europhys. Lett.* **22**, 245 (1993).
- [22] T. V. Ramakrishnan, *Pramana* **22**, 365 (1984).
- [23] M. D. Lipkin, S. A. Rice, and U. Mohanty, *J. Chem. Phys.* **82**, 472 (1985).
- [24] G. L. Jones, *Mol. Phys.* **61**, 455 (1987).
- [25] E. Velasco and P. Tarazona, *Phys. Rev. A* **36**, 979 (1987).
- [26] M. V. Jarić and U. Mohanty, *Phys. Rev. Lett.* **58**, 230 (1987); *Phys. Rev. B* **37**, 4441 (1988).
- [27] H. Xu and M. Baus, *Phys. Rev. A* **38**, 4348 (1988).
- [28] H. Löwen, *J. Phys. Condens. Matter* **2**, 8477 (1990).
- [29] M. Ferconi and M. P. Tosi, *J. Phys. Condens. Matter* **3**, 9943 (1991).
- [30] M. Raj Lakshmi, H. R. Krishnamurthy, and T. V. Ramakrishnan, *Phys. Rev. B* **37**, 1936 (1988).
- [31] R. McRae, J. D. McCoy, and A. D. J. Haymet, *J. Chem. Phys.* **93**, 4281 (1990).
- [32] M. Ferconi and M. P. Tosi, *Europhys. Lett.* **14**, 797 (1991).
- [33] M. C. Mahato, H. R. Krishnamurthy, and T. V. Ramakrishnan, *Phys. Rev. B* **44**, 9944 (1991).
- [34] Y. Rosenfeld, *Phys. Rev. A* **43**, 5424 (1991).
- [35] J.-L. Barrat, J.-P. Hansen, G. Pastore, and E. M. Waisman, *J. Chem. Phys.* **86**, 6360 (1987).
- [36] A. de Kuijper, W. L. Vos, J.-L. Barrat, J.-P. Hansen, and J. A. Schouten, *J. Chem. Phys.* **93**, 5187 (1990).
- [37] B. B. Laird and D. M. Kroll, *Phys. Rev. A* **42**, 4810 (1990).
- [38] D. A. Young and B. J. Alder, *J. Chem. Phys.* **60**, 1254 (1974).
- [39] For a review, see D. Frenkel and J. P. McTague, *Annu. Rev. Phys. Chem.* **31**, 491 (1980).
- [40] R. L. Jacobs, *J. Phys. C* **16**, 273 (1983).
- [41] J. L. Colot, M. Baus, and H. Xu, *Mol. Phys.* **57**, 809 (1986).
- [42] W. A. Curtin and K. J. Runge, *Phys. Rev. A* **35**, 4755 (1987).
- [43] M. Popović and M. V. Jarić, *Phys. Rev. B* **38**, 808 (1988).
- [44] H. C. Longuet-Higgins and B. Widom, *Mol. Phys.* **8**, 549 (1964).
- [45] J. D. Weeks, D. Chandler, and H. C. Andersen, *J. Chem. Phys.* **54**, 5237 (1971).
- [46] M. S. Wertheim, *Phys. Rev. Lett.* **10**, 321 (1963); E. Theile, *J. Chem. Phys.* **39**, 474 (1963).
- [47] J.-P. Hansen and I. R. McDonald, *Theory of Simple Liquids*, 2nd ed. (Academic, London, 1986).
- [48] L. Verlet and J. J. Weis, *Phys. Rev. A* **5**, 939 (1972).
- [49] W. G. Hoover and F. H. Ree, *J. Chem. Phys.* **49**, 3609 (1968); B. J. Alder, W. G. Hoover, and D. A. Young, *ibid.* **49**, 3688 (1968).
- [50] D. Frenkel, *Phys. World* **6**, 24 (1993).
- [51] I. Newton, *Philosophiae Naturalis Principia Mathematica*, 3rd ed. (Apud. Guil. & Joh. Innys, Londini, 1726), Proposition XIX, Theorem XIV; *Sir Isaac Newton's Mathematical Principles of Natural Philosophy and His System of the World*, translated by A. Motte, revised and annotated by F. Cajori (University of California Press, Berkeley, 1934), pp. 300–302. For an interesting discussion, see S. G. Brush, *Statistical Physics and the Atomic Theory of Matter* (Princeton University Press, Princeton, NJ, 1983), pp. 21–23.
- [52] A. R. Denton, P. Nielaba, K. J. Runge, and N. W. Ashcroft, *J. Phys. Condens. Matter* **3**, 593 (1991); *Phys. Rev. Lett.* **64**, 1529 (1990).
- [53] S. Shinomoto, *J. Stat. Phys.* **32**, 105 (1983).
- [54] T. Biben and J.-P. Hansen, *Phys. Rev. Lett.* **66**, 2215 (1991).
- [55] P. D. Kaplan, J. L. Rouke, A. G. Yodh, and D. J. Pine, *Phys. Rev. Lett.* **72**, 582 (1994).
- [56] L. Tonks, *Phys. Rev.* **50**, 955 (1936); J. E. Lennard-Jones and A. F. Devonshire, *Proc. R. Soc. London Ser. A* **163**, 53 (1937); **165**, 1 (1938); **169**, 317 (1939); **170**, 464 (1939); J. G. Kirkwood, *J. Chem. Phys.* **18**, 380 (1950); W. W. Wood, *ibid.* **20**, 1334 (1952); Z. W. Salsburg and W. W. Wood, *ibid.* **37**, 798 (1962).